Dalton Transactions

Accepted Manuscript

ROYAL SOCIETY OF CHEMISTRY

www.rsc.org/dalton

Journal Name

RSCPublishing

ARTICLE

Influence of PNIPAm on log K_f of a copolymerized 2,2'-bipyridine: revised bifunctional ligand design for ratiometric metal-ion sensing

Cite this: DOI: 10.1039/x0xx00000x

Received 00th January 2012,
Accepted 00th January 2012

DOI: 10.1039/x0xx00000x

www.rsc.org/

Justin O. Massing and Roy P. Planalp*

Here we describe the synthesis of a model compound (**1**) based upon a previously reported bifunctional 2,2'-bipyridine (**2**). Ligand pK_a and thermodynamic stability constants were investigated by potentiometric titrations for **1** in order to assess the metal-binding capabilities of **2** following subsequent incorporation within a temperature-responsive polymer that functions as a fluorescent metal-ion indicator. While the log K_{Cu1} measured here was found to be 8.86 ± 0.05 at 25 ºC, this value was previously seen to fall 2.8 orders of magnitude following copolymerization of **2** with poly(*N*-isopropylacrylamide) (PNIPAm). This drop in affinity was attributed to stabilization of the neutral ligand by the polymer environment and elevated temperatures at which metal-binding experiments were performed. ΔH (-54.4 kJ mol^{-1}) and ΔS (-12.8 J K^{-1} mol^{-1}) were therefore determined through variable temperature titrations in order to establish the temperature dependence of log K_{Cu1}. Doing so enabled elucidation of the overall effect that the polymer environment exerts on thermodynamic stability of copolymerized **2**. Specifically, the polymer indicator was found to decrease the thermodynamic stability by 2.2 orders of magnitude, whereas elevated temperatures account for the additional 0.6 order of magnitude drop observed. This finding has implications regarding the design of future bifunctional ligands for ratiometric sensing within our temperature-responsive polymer indicator.

Introduction

Copper's ability to access several oxidation states renders it extremely useful for small molecule activation in living systems.[1, 2] However, copper mismanagement is known to promote oxidative stress, a hallmark of cancer[3] and neurodegeneration.[4] Thus, uptake, trafficking, and storage of this metal within cellular compartments are strictly regulated by membrane transporters, metallochaperones, and metalloregulatory proteins, respectively.[5] Environmental contamination, however, provides an alternate means of disrupting homeostatic control, leading to systemic copper overload and concomitant oxidative stress.[6] While analytical methods (e.g., atomic absorption spectroscopy) are in place to ensure appropriate copper concentrations are maintained, these techniques take into account total concentrations only. The issue here lies in the fact that much of the aqueous copper present is bound by naturally occurring ligands, such as humic and fulvic acids, rendering this metal less bioavailable and substantially less toxic.[7, 8] Therefore, a means of accurately evaluating bioavailable copper levels in water samples is highly desirable, in that it avoids costly and unnecessary treatment of nontoxic bodies of water. Quantifying bioavailable Cu(II), however, remains a challenging task due to its low concentrations. While fluorescence spectroscopy is well suited to address this issue, most fluorescent indicators are restricted to a less desirable turn-off response owing to this metal's paramagnetic nature.[9] And while

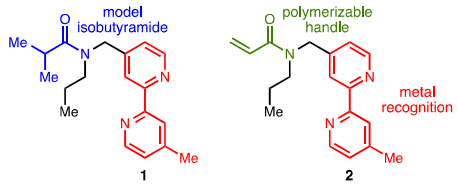

Figure 1. Model bifunctional ligand (**1**) based upon a previously synthesized copolymerizable 2,2'-bipyridine (**2**).

turn-on and ratiometric indicators exist for Cu(II), these sensors too are limited by poor water solubility[10] and irreversibility.[11]

To address these issues, we recently reported a water-soluble polymer indicator capable of sensing paramagnetic metals ratiometrically.[12-14] We achieved this by physically separating metal recognition from the fluorescence response along a temperature-responsive polymer. Poly(*N*-isopropylacrylamide) (PNIPAm) was chosen due to its well-defined structural transition from an expanded coil to a collapsed globule at 32 ºC. This lower critical solution temperature (LCST) may be systematically raised and lowered by increasing hydrophilic and hydrophobic interactions, respectively.[15] For instance, incorporating a charge-neutral ligand (e.g., 2,2'-bipyridine) would serve to lower the LCST. Binding of cationic species, however, elevates the LCST by

introducing charge along the polymer backbone, thereby causing the polymer to expand when temperature is held constant. Incorporation of a donor and acceptor fluorophore pair within this scaffold permits interrogation of the polymer structure, which may then be correlated with bioavailable metal concentrations (Fig. 2). We have therefore initiated a research program dedicated to the rational design and development of bifunctional ligands capable of modulating these macromolecular transformations through metal coordination.

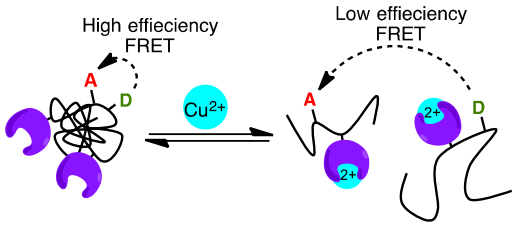

Figure 2. Incorporation of a charge-neutral ligand within temperature-responsive PNIPAm depresses its LCST, yielding a collapsed globule above this temperature. This conformation facilitates efficient energy transfer between a donor and acceptor fluorophore pair. When temperature is held constant, metal coordination affords polymer expansion and a concomitant decrease in energy transfer. This design provides a modular platform for ratiometric sensing of any metal through rational design of the corresponding bifunctional ligand.

Our group has designed and synthesized a variety of bifunctional ligands bearing both a polymerizable acrylamide and a chelating functionality. In order to characterize the metal binding capabilities of these compounds, we also synthesize the isobutyramide analogues that more closely resemble these agents following copolymerization with NIPAm (Fig. 1). Here we report the synthesis of an isobutyramide analogue (**1**) of a previously reported bifunctional 2,2'-bipyridine (**2**). We then evaluated the pK_a and thermodynamic stability constants of **1** by potentiometric titrations. Moreover, we determined thermodynamic parameters (ΔH and ΔS) relevant to formation of the Cu**1**$^{2+}$ complex to better understand the effect temperature and the polymer environment exert on **2** following incorporation within our indicator system.

Experimental methods

All reactions were performed under nitrogen atmosphere in flame-dried glassware equipped with a magnetic stir bar unless otherwise stated. Formation of 4'-methyl-[2,2'-bipyridine]-4-carbaldehyde (**4**) from 4,4'-dimethyl-2,2'-bipyridine (**3**) was achieved as previously reported.[16] Anhydrous solvents were obtained from an Innovative Technology Inc. Solvent Delivery System. ^{1}H NMR spectra were recorded on a Varian Mercury 400 MHz NMR spectrometer and are reported in ppm relative to the deuterated solvent used ($CDCl_3$ at 7.26 ppm). Spectral data are reported as s = singlet, d = doublet, t = triplet, q = quartet, p = pentet, hept = heptet, m = multiplet; coupling constant(s) in Hz; integration. Proton-decoupled ^{13}C NMR spectra were recorded on a Varian Mercury 400 (101 MHz) NMR spectrometer and are reported in ppm relative to the deuterated solvent used ($CDCl_3$ at 77.16 ppm). Mass spectra data were obtained on either a JEOL accuTOF DART mass spectrometer or Bruker amaZon SL ion trap LC/MS. Potentiometric titrations were performed using a 785 DMP Titrino equipped with an Accumet double junction pH electrode and thermally-regulated titration vessel maintained at either 278, 298, or 318 K. Samples were prepared using freshly degassed water and the ionic strength adjusted to 0.1 M with $NaNO_3$. Samples were purged with N_2 prior to measurement, while an inert atmosphere previously saturated with 0.1 M $NaNO_3$ was maintained throughout the course of the experiment. Data were analyzed using Hyperquad2008,[17] while the autoprotolysis constant of H_2O was defined as 14.43, 13.77, and 13.34 at 278, 298, and 318 K, respectively. Distribution diagrams were generated using HySS 2008.

Synthesis

***N*-((4'-methyl-[2,2'-bipyridin]-4-yl)methylene)propan-1-amine (5).** To a solution of **4** (2.832 g, 14.29 mmol) in DCM (60 mL) were added finely powdered 3 Å molecular sieves (2.4 g), followed by n-propylamine (1.75 mL, 21.4 mmol) dropwise. The reaction mixture was allowed to stir at room temperature under N_2 for 30 h before filtering through Celite. The filtrate was concentrated under reduced pressure to afford **5** as a pale yellow oil (3.364 g, 98%). ^{1}H NMR (400 MHz, $CDCl_3$) δ 8.74 – 8.70 (m, 1H), 8.60 (dd, *J* = 1.7, 0.8 Hz, 1H), 8.56 – 8.53 (m, 1H), 8.33 (d, *J* = 1.4 Hz, 1H), 8.24 (dt, *J* = 1.7, 0.8 Hz, 1H), 7.70 (dd, *J* = 5.0, 1.6 Hz, 1H), 7.13 (ddd, *J* = 5.1, 1.7, 0.8 Hz, 1H), 3.63 (td, *J* = 6.9, 1.4 Hz, 2H), 2.42 (d, *J* = 0.7 Hz, 3H), 1.75 (h, *J* = 7.2 Hz, 2H), 0.96 (t, *J* = 7.4 Hz, 3H). ^{13}C NMR (101 MHz, $CDCl_3$) δ 159.28, 157.27, 155.62, 149.72, 149.20, 148.30, 144.37, 125.09, 122.13, 121.08, 120.68, 63.86, 24.01, 21.38, 12.05; HRMS (ESI): Exact mass cald. For $C_{15}H_{17}N_3$ $[M+H]^+$, 240.1501. Found 240.1482.

***N*-((4'-methyl-[2,2'-bipyridin]-4-yl)methyl)propan-1-amine (6). 5** (3.283 g, 13.72 mmol) was dissolved in MeOH (60 mL). $NaBH_4$ (1.342 g 35.48 mmol) was added to the stirred solution, affording vigorous effervescence. Stirring was continued under N_2 for 18 h followed by concentration under reduced pressure. The resulting pale yellow residue was then dissolved in H_2O (100 mL), made basic by addition of 1.0 M $NaOH_{(aq)}$ (pH = 11 as evidenced by paper), and extracted with DCM (5 x 10 mL). The combined organic fractions were dried over Na_2SO_4 and concentrated under reduced pressure to a colorless oil (3.136 g, 95%). ^{1}H NMR (400 MHz, $CDCl_3$) δ 8.62 (dd, *J* = 5.0, 0.7 Hz 1H), 8.54 (dd, *J* = 5.0, 0.7 Hz, 1H), 8.32 (dd, *J* = 1.7, 0.8 Hz, 1H), 8.23 (dt, *J* = 1.6, 0.8 Hz, 1H), 7.33 (ddt, *J* = 5.1, 1.6, 0.7 Hz, 1H), 7.13 (ddd, *J* = 5.0, 1.7, 0.8 Hz, 1H), 3.89 (s, 2H), 2.67 – 2.55 (m, 2H), 2.44 (s, 3H), 1.54 (h, *J* = 7.4 Hz, 2H), 0.93 (t, *J* = 7.4 Hz, 3H).^{13}C NMR (101 MHz, $CDCl_3$) δ 156.49, 156.16, 150.99, 149.41, 149.15, 148.33, 124.89, 123.19, 122.22, 120.67, 53.15, 51.62, 23.43, 21.39, 11.97; HRMS (ESI): Exact mass cald. For $C_{15}H_{19}N_3$ $[M+H]^+$, 242.1657. Found 242.1650.

***N*-((4'-methyl-[2,2'-bipyridin]-4-yl)methyl)-*N*-propylacrylamide (2).** Et_3N (0.50 mL, 3.6 mmol) and **6** (0.289 g, 1.20 mmol) were dissolved in DCM (15 mL) and allowed to stir for 10 min at 0 ºC before adding acryloyl chloride (0.11 mL, 1.4 mmol). The reaction mixture was allowed to slowly warm to room temperature with continued stirring for 12 h under N_2. The reaction mixture was filtered through Celite and washed with 0.1 M $HCl_{(aq)}$ (2 x 50 mL). The aqueous layer was extracted with DCM (3 x 25 mL), and the organic fractions combined, dried over Na_2SO_4, and concentrated under reduced pressure to yield **2** as a yellow oil (0.182 g, 51%). ^{1}H NMR (400 MHz, $CDCl_3$) δ 8.65 (d, *J* = 5.1 Hz, 1H), 8.61 (d, *J* = 4.9 Hz, 2H), 8.54 (dd, *J* = 5.0, 0.8 Hz, 3H), 8.25 (d, *J* = 14.0 Hz, 6H), 7.25 – 7.19 (m, 2H), 7.19 – 7.11 (m, 4H), 6.67 (dd, *J* = 16.7, 10.3 Hz, 2H), 6.50 (d, *J* = 2.1 Hz, 1H), 6.44 (dt, *J* = 10.6, 2.0 Hz, 3H), 5.79 (dd, *J* = 10.3, 2.1 Hz, 2H), 5.67 (dd, *J* = 8.6,

3.7 Hz, 1H), 4.76 (s, 4H), 4.69 (s, 2H), 3.49 – 3.42 (m, 2H), 3.37 – 3.30 (m, 4H), 2.45 (s, 9H), 1.71 – 1.57 (m, 6H), 0.92 (td, J = 7.6, 3.5 Hz, 9H). ^{13}C NMR (101 MHz, $CDCl_3$) δ 167.01, 166.91, 157.04, 156.57, 155.83, 155.53, 149.98, 149.68, 149.23, 149.08, 148.55, 148.20, 147.90, 129.18, 127.73, 127.32, 125.24, 125.06, 122.74, 122.35, 121.16, 120.39, 119.19, 50.84, 49.91, 48.99, 22.71, 21.44, 21.09, 11.62, 11.37; HRMS (ESI): Exact mass cald. For $C_{18}H_{21}N_3O$ $[M+H]^+$, 296.1763. Found 296.1714.

***N*-((4'-methyl-[2,2'-bipyridin]-4-yl)methyl)-*N*-propylisobutyramide (1).** **6** (1.434 g, 5.942 mmol) and Et_3N (1.793 g, 17.72 mmol) were dissolved in DCM (40 mL) and allowed to stir for 10 min at 0 ºC before adding isobutyryl chloride (0.67 mL, 6.4 mmol). The reaction was allowed to warm to room temperature and continue stirring under N_2. After 24 h the reaction mixture was filtered through Celite, washed with 0.1 M $HCl_{(aq)}$ (3 x 50 mL), and combined organic fractions dried over Na_2SO_4. The pale yellow solution was then concentrated under reduced pressure to a peach colored residue (1.756 g, 95%). ^{1}H NMR (400 MHz, $CDCl_3$) δ 8.68 – 8.64 (m, 1H), 8.62 – 8.58 (m, 2H), 8.56 – 8.51 (m, 3H), 8.27 (dd, J = 1.8, 0.9 Hz, 1H), 8.23 (dd, J = 2.0, 1.0 Hz, 3H), 8.23 – 8.21 (m, 2H), 7.19 – 7.07 (m, 6H), 4.69 (s, 4H), 4.65 (s, 2H), 3.43 – 3.36 (m, 2H), 3.31 – 3.23 (m, 4H), 2.90 (hept, J = 6.7 Hz, 2H), 2.65 (hept, J = 6.5 Hz, 1H), 2.45 (s, 3H), 2.44 (s, 6H), 1.68 – 1.52 (m, 6H), 1.23 (d, J = 6.7 Hz, 12H), 1.12 (d, J = 6.7 Hz, 6H), 0.90 (q, J = 7.3 Hz, 9H). ^{13}C NMR (101 MHz, $CDCl_3$) δ 177.88, 177.81, 157.06, 156.62, 155.95, 155.58, 149.92, 149.63, 149.27, 149.17, 148.67, 148.46, 148.36, 125.21, 124.98, 122.33, 122.24, 120.89, 120.21, 119.09, 50.47, 49.60, 48.48, 48.22, 30.85, 30.36, 22.70, 21.40, 21.06, 20.04, 19.93, 11.50, 11.37; LC/MS (ESI): Exact mass cald. For $C_{19}H_{25}N_3O$ $[M+H]^+$, 312.2076. Found 312.2461.

Results and discussion

Initial oxidation of 4,4'-dimethyl-2,2'-bipyridine (**3**) with SeO_2 yielded the desired aldehyde (**4**) in addition to the undesired carboxylic acid (Scheme 1). Pure **4** was obtained in 36% yield through formation of a water-soluble sulfonate adduct with $NaHSO_{3(aq)}$ that was then liberated at elevated pH values and subsequently extracted into DCM. Condensation between **4** and propylamine cleanly afforded the desired imine product **5** in 98% yield, followed by reduction with $NaBH_4$ to generate the penultimate amine **6** in 95% yield.[13] Amide formation at 0 ºC with either isobutyryl or acryloyl chloride in the presence of Et_3N provided the corresponding isobutyramide (**1**) and acrylamide (**2**) derivatives in 95% and 51% yield, respectively.

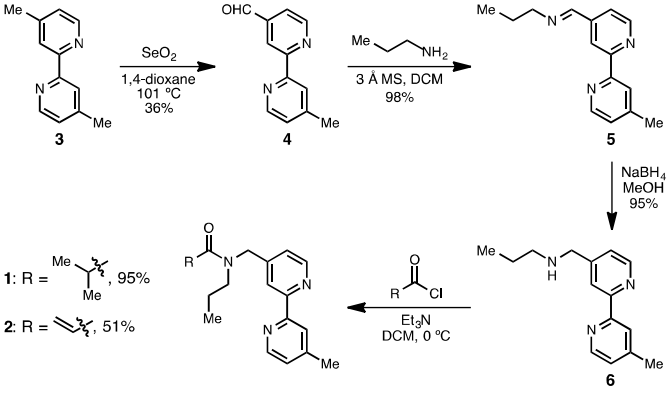

Scheme 1. Synthesis of copolymerizable **2** and model compound **1**

Further, both **1** and **2** exist as a 2:1 mixture of rotamers as evidenced by the ^{1}H NMR spectra. pK_a and thermodynamic stability constants for **1** were then investigated by potentiometric titrations, whereas **2** was copolymerized and its ability to quantify metal-ion concentrations in wastewater samples evaluated.[13]

We initially interrogatted the pK_a value of **1** (Fig. 3), which we found to be 4.81. This value is somewhat elevated relative to that seen for 2,2'-bipyridine (4.41),[18] and may be reasoned

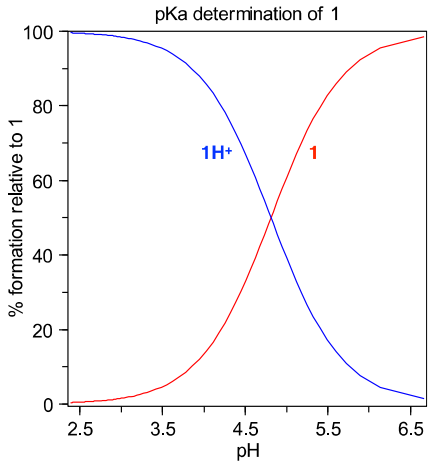

Figure 3. pH profile of **1** + 3 mol equiv. HNO_3 ([**1**] = 1.9 mM, 25 ºC, I = 0.1 M $NaNO_3$).

through inductive contributions from the 4 and 4' alkyl substituents. Owing to the weakly basic nature of **1**, there is poor competition between protons and metal for this ligand. Thus, at acidic pH, **1** would largely exist as metallated species, thereby complicating thermodynamic stability determination. It was therefore necessary to perform potentiometric titrations in the presence of tris(2-aminoethyl)amine (TREN) (eq. 1).[19, 20]

$$M(\mathbf{1})_x^{2+} + TRENH_3^{3+} \rightleftharpoons MTREN^{2+} + \mathbf{1}H^+ + 2H^+ \qquad (1)$$

We independently characterized this competing ligand's pK_a and thermodynamic stability constants with Cu(II), Ni(II), and Zn(II). Ni(II) and Zn(II) were included owing to their interferring nature in wastewater samples. Values obtained were found to be in good agreement with those reported in the

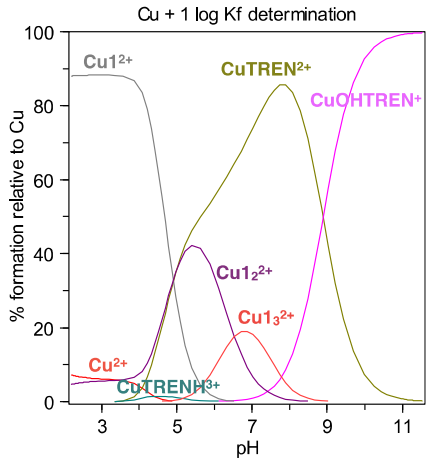

Figure 4. Distribution diagram for 1:1:1 Cu(II):**1**:TREN·3HCl mixture ([Cu] = [**1**] = [TREN·3HCl] = 1.8 mM, 25 ºC, I = 0.1 M $NaNO_3$).

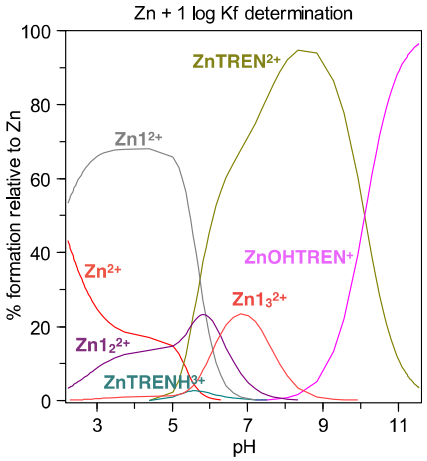

Figure 5. Distribution diagram for 1:1:1 Zn(II):**1**:TREN·3HCl mixture ([Zn] = [**1**] = [TREN·3HCl] = 1.8 mM, 25 ºC, I = 0.1 M $NaNO_3$).

literature.[18] Again, as previously stated, the weak basicity of **1** necessitated the use of TREN as a competing ligand during subsequent titrations conducted in the presence of metal ions. Below a pH of 4, Cu(II) is largely sequestered as Cu**1**$^{2+}$ with a log K_f of 8.86 (Fig. 4). This value, as expected, is elevated with respect to the analagous complex between Cu(II) and 2,2'-bipyridine (8.12)[18] given the heightend basicity of **1**. Raising the pH serves to deprotonate TREN, thereby allowing this tetradentate ligand to efficiently bind Cu(II). The amount of CuTREN^{2+} steadily increases between a pH of 4 and 8 and quickly drops after this due to formation of the CuOHTREN^{+} species. Moreover, formation of CuTREN^{2+} between this pH range is accompanied by appearance of Cu**1**$_2^{2+}$ and Cu**1**$_3^{2+}$ with log K_f values of 5.66 and 3.71, respectively. These values too were found to be in good agreement with those reported for the analagous 2,2'-bipyridine species (log K_{CuL2} = 5.51; log K_{CuL3} = 3.4).[18] Zn(II) was found to exhibit a similar speciation profile (Fig. 5); formation constants between our model ligand and this metal are presented in Table 1.

Though Ni(II) is similar to Cu(II) and Zn(II), we were unable to detect a NiOHTREN^{+} species during potentiometric titrations between Ni(II), TREN, and **1** (Fig. 6). Below a pH of 4, 60% and 20% of Ni(II) is bound as the mono (log K_{Ni1} = 7.47) and bis species (log K_{Ni12} = 6.52), respectively, while the remaining 20% is free Ni(II) in solution. At neutral pH,

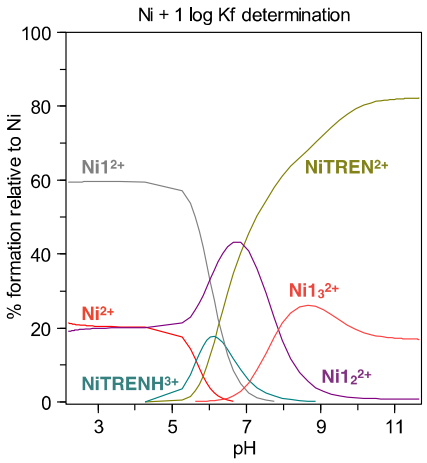

Figure 6. Distribution diagram for 1:1:1 Ni(II):**1**:TREN·3HCl mixture ([Ni] = [**1**] = [TREN·3HCl] = 1.8 mM, 25 ºC, I = 0.1 M $NaNO_3$).

Table 1. Protonation and formation constants for **1** and 2,2'-bipyridine with Ni(II), Cu(II), and Zn(II) (I = 0.1 M, 25 ºC).

	1	**2,2'-bipyridine**[18]
log K_{LH}	4.86 ± 0.03	4.41 ± 0.04
log K_{NiL}	7.47 ± 0.08	7.04 ± 0.03
log K_{NiL2}	6.52 ± 0.08	6.82 ± 0.09
log K_{NiL3}	4.40 ± 0.06	6.30 ± 0.03
log K_{CuL}	8.86 ± 0.05	8.12 ± 0.03
log K_{CuL2}	5.67 ± 0.02	5.51 ± 0.03
log K_{CuL3}	3.71 ± 0.01	3.4 ± 0.1
log K_{ZnL}	5.8 ± 0.1	5.12 ± 0.09
log K_{ZnL2}	4.5 ± 0. 1	4.51 ± 0.04
log K_{ZnL3}	4.11 ± 0.08	3.7 ± 0.1

however, Ni(II) exists as equal amounts of Ni**1**$_2^{2+}$ and NiTREN (c. 43% each) while the remaining metal is complexed as either Ni**1**$_3^{2+}$ (log K_{Ni13} = 4.40) or NiTRENH^{3+}. Increasing the pH beyond this point yields a decrease in Ni**1**$_2^{2+}$ and NiTRENH^{3+}, whereas Ni**1**$_3^{2+}$ and NiTREN^{2+} steadily increase and eventually plateau at pH 11.

Thermodynamic stability constants reported in Table 1 for Ni(II), Cu(II), and Zn(II) were found to be in agreement with the Irving-Williams series (Ni(II) < Cu(II) >> Zn(II)) as was expected. Furthermore, these numbers compare well with those previously reported for 2,2'-bipyridine.[18]

Although we have synthesized and characterized the thermodynamic stability between Cu(II) and **1**, the values obtained for this model compound do not accurately translate to those observed with the polymer indicator incorporating **2**. Previous copolymerization of **2** and PNIPAm was found to depress the log K_f by nearly three orders of magnitude.[13] Moreover, formation of the bis and tris chelates seen here were unobserved in the polymer indicator given the low percentage (2%) of **2** incorporated within PNIPAm. While the apparent drop in thermodynamic stability was attributed to globular PNIPAm (hydrophobic) stabilizing the neutral ligand relative to the charged complex, the effect of performing experiments at 45 ºC on the log K_f was not considered. Metal coordination is an exothermic process, and should therefore result in decreased affinity at elevated temperatures. We therefore evaluated the temperature dependence of log K_{Cu1} through a series of variable temperature titrations and Van 't Hoff plots. Doing so enabled the effect of the polymer environment on thermodynamic stability to be evaluated.

The first three pK_a values for TREN were determined at 278, 298, and 318 K, and are presented in Table 2. Plotting the ln K_{eq} against 1/T yielded the corresponding linear Van 't Hoff plots (supplemental material). Multiplying the negative slope and intercept by the gas constant (R = 8.314 J K^{-1} mol^{-1}) gave ΔH and ΔS, respectively (Table 2). Obtained values were found to be in agreement with those reported in the literature. Log K_f values between Cu(II) and TREN were similarly established at these three separate temperatures. The CuOHTREN^{+} species was not included in this analysis as it does not exist at pH values relevant to the formation of Cu**1**$^{2+}$ seen here. Potentiometric titrations were then performed to elucidate the pK_a value of **1** at 278, 298, and 318 K, followed by determination of its thermodynamic stability constant with an equivalent of Cu(II) at these temperatures. Plotting the ln K_{eq} of the latter against 1/T afforded the corresponding Van 't Hoff

Table 2. Protonation and formation constants for TREN and **1** with Cu(II) at 278, 298, and 318 K (I = 0.1 M) and the corresponding ΔH and ΔS values.

		278 K	298 K	318 K	ΔH (kJ mol^{-1})	ΔS (J K^{-1} mol^{-1})
TREN	log K_{LH}	10.65 ± 0.02	10.12 ± 0.04	9.62 ± 0.01	-43.5 (-47.2)[a]	47.4 (35)[a]
	log K_{LH2}	10.23 ± 0.01	9.51 ± 0.02	8.96 ± 0.01	-52.6 (-53.6)[a]	5.9 (-0.4)[a]
	log K_{LH3}	9.17 ± 0.01	8.6 ± 0.2	7.88 ± 0.01	-59.3 (-54.5)[a]	-35.8 (-15)[a]
	log K_{CuL}	20.17 ± 0.02	18.75 ± 0.04	17.84 ± 0.01	-99.0 (-99.0)[a]	28.8 (73.6)[a]
	log K_{CuLH}	3.77 ± 0.03	3.59 ± 0.01	3.42 ± 0.03	-14.7	19.4
1	log K_{LH}	5.013 ± 0.009	4.86 ± 0.03	4.724 ± 0.004	-12.2 (-15)[b]	52.0 (32)[b]
	log K_{CuL}	9.56 ± 0.03	8.86 ± 0.05	8.28 ± 0.03	-54.4 (-46.0)[b]	-12.8 (-13)[b]

[a]Literature values for TREN. [b]Literature values for 2,2'-bipyridine.

plot illustrating the temperature dependence of log K_{Cu1} (Fig. 7). Data refinement at each temperature was carried out using the necessary constants obtained at the corresponding values. As expected, protonation and complexation are exothermic processess and are therefore characterized by a negative ΔH. Furthermore, increasing the temperature from 298 to 318 K was found to lower the log K_{Cu1} more than half an order of magnitude. This observation, in combination with the hydrophobic PNIPAm environment further explains the marked decrease in log K_{Cu2} recognized following copolymerization. Thus, in the case of copolymerized **2**, the PNIPAm

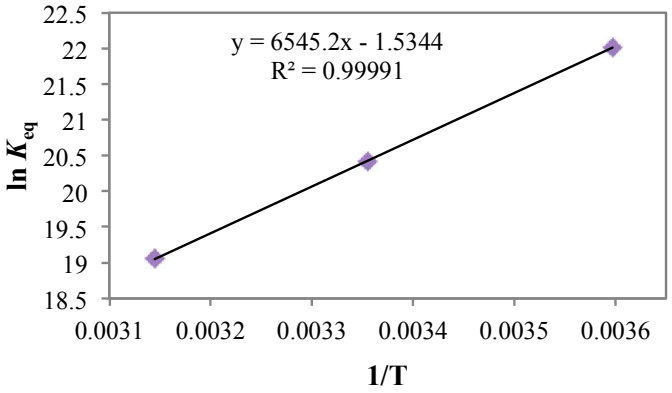

Figure 7. Cu**1**$^{2+}$ Van 't Hoff plot.

environment was found to effectively lower the log K_f by 2.2 orders of magnitude as opposed to 2.8. Future ligand designs will therefore account for this observation.

Conclusions

In summary, we have synthesized a bifunctional ligand (**2**) and its isobutyramide analogue (**1**), and evaluated the latter's metal binding abilities. The former compound was previously incorporated within a temperature-responsive polymer able to ratiometrically sense aqueous Cu(II).[13] The log K_f of **2** copolymerized with PNIPAm was seen to fall nearly three orders of magnitude relative to that value measured for **1** here at 45 ºC. We therefore established the temperature dependence of log K_{Cu1} to better understand the degree to which PNIPAm influences the thermodynamic stability of copolymerized ligands with metal-ion contaminants. In the case of **2**, it was found that PNIPAm depresses log K_{Cu2} by 2.2 orders of magnitude relative to the model **1** evaluated here. This finding has implications regarding the design of future bifunctional ligands to be incorporated within our polymer-based indicator. Furthermore, this modular sensing platform enables any metal ion of any oxidation state to be accurately detected through rational design of the appropriate bifunctional ligand.[21]

Acknowledgements

We gratefully acknowledge the National Science Foundation (CHE-1012897) and the University of New Hampshire (DYF) for financial support.

Notes and references

Department of Chemistry, University of New Hampshire, Durham, NH 03824, USA. E-mail: roy.planalp@unh.edu

1. I. Bertini, H. B. Gray, E. I. Stiefel, J. S. Valentine, *Biological Inorganic Chemistry: Structure and Reactivity*, University Science Books, Sausalito, CA, 2007.
2. M. R. Halvagar, P. V. Solntsev, H. Lim, B. Hedman, K. O. Hodgson, E. I. Solomon, C. J. Cramer, W. B. Tolman, *J. Am. Chem. Soc.* 2014, **136,** 7269.
3. T. Finkel, M. Serrano, M. A. Blasco, *Nature* 2007, **448,** 767.
4. K. J. Barnham, C. L. Masters, A. I. Bush, *Nat. Rev. Drug. Discov.* 2004, **3,** 205.
5. A. K. Boal, A. C. Rosenzweig, *Chem. Rev.* 2009, **109,** 4760.
6. C. A. Flemming, J. T. Trevors, *Water, Air, Soil Pollut.* 1989, **44,** 143.
7. M. S. Shuman, J. L. Cromer, *Environ. Sci. Technol.* 1979, **13,** 543.
8. D. M. Di Toro, H. E. Allen, H. L. Bergman, J. S. Meyer, P. R. Paquin, R. C. Santore, *Environ. Toxicol. Chem.* 2001, **20,** 2383.
9. R. Bergonzi, L. Fabbrizzi, M. Licchelli, C. Mangano, *Coord. Chem. Rev.* 1998, **170,** 31.
10. S. Goswami, S. Maity, A. C. Maity, A. K. Maity, A. K. Das, P. Saha, *RSC Advances* 2014, **4,** 6300.
11. Z. Shi, X. Tang, X. Zhou, J. Cheng, Q. Han, J.-a. Zhou, B. Wang, Y. Yang, W. Liu, D. Bai, *Inorg. Chem.* 2013, **52,** 12668.
12. J. Du, S. Yao, W. R. Seitz, N. E. Bencivenga, J. O. Massing, R. P. Planalp, R. K. Jackson, D. P. Kennedy, S. C. Burdette, *Analyst* 2011, **136,** 5006.
13. S. Yao, A. M. Jones, J. Du, R. K. Jackson, J. O. Massing, D. P. Kennedy, N. E. Bencivenga, R. P. Planalp, S. C. Burdette, W. R. Seitz, *Analyst* 2012, **137,** 4734.
14. J. Osambo, W. Seitz, D. Kennedy, R. Planalp, A. Jones, R. Jackson, S. Burdette, *Sensors* 2013, **13,** 1341.
15. H. Feil, Y. H. Bae, J. Feijen, S. W. Kim, *Macromolecules* 1993, **26,** 2496.
16. G. F. Strouse, J. R. Schoonover, R. Duesing, S. Boyde, W. E. Jones, Jr., T. J. Meyer, *Inorg. Chem.* 1995, **34,** 473.
17. P. Gans, A. Sabatini, A. Vacca, *Talanta* 1996, **43,** 1739.
18. A. E. Martell, R. M. Smith. *NIST Critically Selected Stability Constants of Metal Complexes*, Version 8.0, National Institute of Science and Technology (NIST), Gaithersburg, MD, 2004.
19. H. Ackermann, G. Schwarzenbach, *Helv. Chim. Acta.* 1949, **32,** 1543.
20. R. Nakon, P. R. Rechani, R. J. Angelici, *J. Am. Chem. Soc.* 1974, **96,** 2117.
21. J. O. Massing, R. P. Planalp, *Tetrahedron Lett.* in press.

Journal Name RSCPublishing

ARTICLE

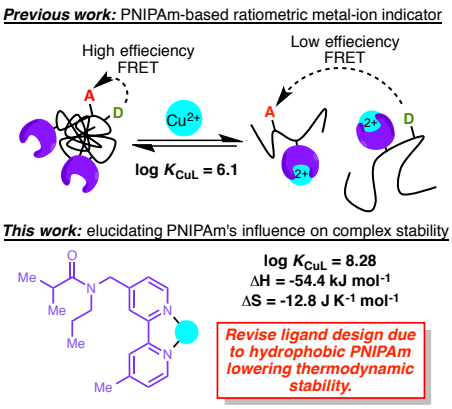

We evaluate the effects of temperature and hydrophobicity on metal-ion sensing within a temperature-responsive indicator for environmental sensing applications.